Size-Controlled Preparation of Polyethylene Nanoplastic Particles by Nanoprecipitation and Insights into the Underlying Mechanisms

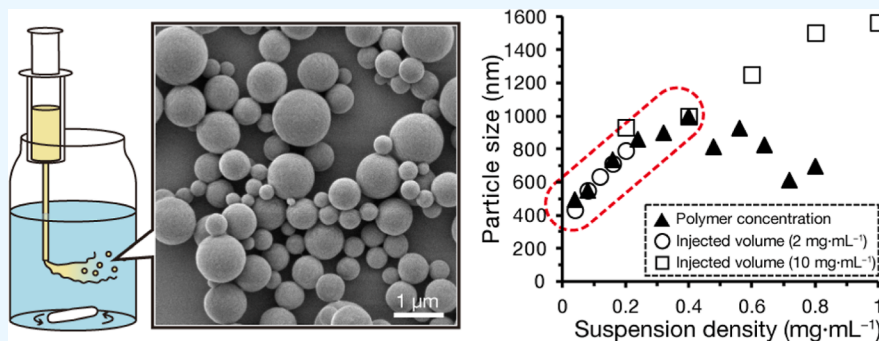Kosuke Tanaka,* Hidetoshi Kuramochi, Kouji Maeda, Yusuke Takahashi, Masahiro Osako, and Go Suzuki

ACCESS | 📊 Metrics & More | 📰 Article Recommendations | 🔵 Supporting Information

ABSTRACT: Plastic pollution is ubiquitous in the environment, and nanoplastics (<1 μm) are of growing concern as they pose more health risks than larger particles. However, because of a lack of appropriate model particles, studies examining the risks of polyolefin nanoplastics are very limited, despite the prevalence of these plastics in the environment. Although nanoprecipitation using organic solvents is a promising method for preparing model nanoplastic particles of polyolefins, there are currently no methods for controlling the particle size. Here, we examined how the concentration and volume of the feedstock polymer solution affect the size of polyethylene particles produced by nanoprecipitation. The mechanisms underlying the particle formation were investigated by using a simple population balance model. Increasing the concentration of the feedstock solution increased the growth rate and decreased the nucleation rate, and increasing the volume of the feedstock solution increased the growth rate, resulting in an increase in the mean particle diameter in both cases. These changes in particle diameter were linearly correlated with the suspension density of the dispersion up to a suspension density of 0.4 mg·mL^{-1}. In addition, at these suspension densities, spherical particles were prepared without generating aggregates. Together, these results show that the diameter of polyethylene particles prepared by nanoprecipitation could be controlled according to the suspension density up to a suspension density of 0.4 mg·mL^{-1}. This study provides a basis for the development of nanoprecipitation-based techniques for the precise, scale-independent production of model nanoplastic particles, which we hope will accelerate the risk assessment of nanoplastics.

■ INTRODUCTION

Microplastic (particle diameter, < 5 mm) pollution is ubiquitous in the environment and an important environmental concern worldwide. The largest source of microplastics is the weathering and fragmentation of larger plastic debris already in the environment.[1] The fragmentation process most likely produces not only microplastics but also fragments smaller than microplastics, called nanoplastics (NPs), which are defined as plastic particles with sizes on the nanometer scale (1−1000 nm).[2] Recent studies have confirmed not only the presence of NPs in the environment but also humans are exposed to these NPs.[3,4]

Microplastics are generally unable to cross biological barriers, such as those of the gut or lung, and are therefore not absorbed by most organisms.[5] However, smaller particles that are a few micrometers in size can cross those barriers, and

NPs that fall within this size range have been found to easily enter the bodies of organisms.[6] Experimental evidence of the dangers of NPs, such as their potential to induce oxidative stress and inflammatory reactions, is accumulating.[7,8] However, most of the risk assessments performed to date have examined polystyrene NPs because commercial model particles are easily obtained.[9] This has meant that other types of plastics, for which there are no commercial model particles available, such as the polyolefins polyethylene and polypropylene, have largely

been ignored despite the prevalence of these plastics in the environment. Of the studies that are available, several examinations of the toxicity of polyethylene NPs produced by the mechanical breakdown of larger plastics have been reported recently: Baudrimont et al. reported that polyethylene NPs collected from the North Atlantic Ocean inhibit the growth of the freshwater green alga *Scenedesmus subspicatus*; Arini et al. reported that exposure to polyethylene NPs causes cardiovascular toxicity, such as pericardial edema and cardiac output, in zebrafish embryos; and Ekvall et al. reported that only the NP fraction smaller than 3 nm is toxic in *Daphnia magna* and that the observed toxicity is caused by additives and short-chain polyethylenes that have leached from the NPs.[10−12]

Previously, we reported a nanoprecipitation-based method for preparing nanoscale particles of five major polymers, including three polyolefins [i.e., low-density polyethylene (LDPE), high-density PE, and polypropylene].[13] Nanoprecipitation has been used to prepare nanoparticles of biodegradable polymers, such as polylactic acid, for use as a drug delivery medium, but the number of studies about nanoprecipitation of other polymers, including polyolefins, is limited.[14,15] Because the method we developed does not use additives such as surfactants, it affords particles without impurities that could induce adverse effects in organisms. In addition, the particles prepared by our method have molecular weight distributions, crystallinities, and thermal properties that are comparable with those of commercial polymers; therefore, they are appropriate for use as model particles. Although our method produces only spherical particles, which are in contrast to the irregular shapes of NPs found in the environment, the sphere is the simplest uniform shape, meaning the particles can be standardized. These points make these particles a fundamental reference material with which to explore the effects of different morphological features on toxicity. Recently, other groups have also reported precipitation-based methods to prepare polyolefin NPs.[16−18] Although nanoprecipitation-based methods are a promising means of producing model NP particles, there are currently no approaches for controlling the size of the particles that are obtained. Producing particles of specific sizes is important for conducting risk assessments because particle size is directly related to the adsorption of particles by organisms and the physical behaviors of particles in the environment.[6] Therefore, methods to control the size of particles produced by nanoprecipitation are needed.

Here, we examined how varying the concentration and volume of the polymer feedstock solution affects the diameter of LDPE particles prepared by nanoprecipitation. In addition, the underlying mechanisms were investigated based on crystallization. The driving force of crystallization is supersaturation in which dissolved polymer is "pushed out" from a saturated solution. This "pushing out" occurs via nucleation and growth. In this study, to investigate growth rate and nucleation rate during nanoprecipitation, we used a simple population balance model, which is a common means of simulating the size distribution and other properties of particulate systems.[19]
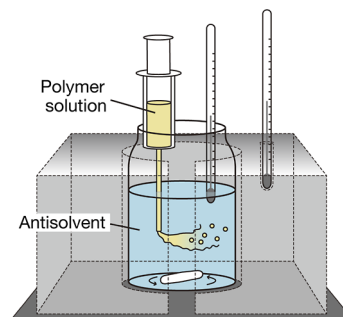
EXPERIMENTAL SECTION

Materials. LDPE sheets were purchased from Kokugo Co., Ltd., Tokyo, Japan (cat. no. 107-12402). The number-average and weight-average molecular weights were 18.1 and 81.2, respectively, and the degree of crystallinity and melting

temperature were 41.4% and 107.0 °C, respectively;[13] these parameters were all within the ranges reported in the literature for commercial polymers.[13]

NANOPRECIPITATION

Nanoprecipitation was conducted as previously reported (Figure 1).[13] The experimental conditions used in the present

Figure 1. Schematic overview of the preparation of LDPE particles by nanoprecipitation.

Table 1. Experimental Conditions[a]

variable	LDPE concentration in feedstock solution	volume of injected feedstock solution
temperature (°C)	110	110
stirring rate (rpm)	1000	1000
LDPE concentration (mg·mL^{-1})	1, 2, 4, 6, 8, 10, 12, 14, 16, 18, 20, 30, 40	2, 10
injected volume (mL)	4	2, 4, 6, 8, 10
residence time (s)	13	13
rate of injection (mL·s^{-1})	0.31	0.15−0.77

[a]LDPE, low-density polyethylene.

study are listed in Table 1. The LDPE sheets were dissolved in xylene at 110 °C. The antisolvent for precipitation was 100 mL of dimethyl sulfoxide (DMSO) placed in a 100 mL glass bottle. The feedstock solution was injected into the antisolvent via a disposable glass pipette, with stirring by a magnetic stir bar set at 1000 rpm. Although a recent study of polystyrene nanoprecipitation has reported dependence of particle formation on the rate of mixing,[20] we did not find that stirring rate (500−1500 rpm) had an effect on particle size under the present experimental conditions (Figure S1). We therefore set the stirring rate at 1000 rpm and excluded stirring rate from consideration as a determinant of particle size. The operative variables were the concentration of LDPE in the feedstock solution (1, 2, 4, 6, 8, 10, 12, 14, 16, 18, 20, 30, 40 mg·mL^{-1}, with 4 mL of feedstock solution used) and the volume of the feedstock solution injected (2, 4, 6, 8, or 10 mL, at a polymer concentration of 2 or 10 mg·mL^{-1}). After injection of the feedstock solution into the antisolvent, the bottle was immediately cooled with water to room temperature (≈20 °C). After cooling, the contents of the bottle were passed through a stainless-steel net with a mesh size of 0.25 mm to remove large aggregates. Then, the particles in the filtrate were collected by filtration using a polyester track-etched membrane filter with 0.2 μm pore size (cat. no. 1215288; GVS S.p.A.,

Bologna, Italy). Particles collected on the membrane filter were washed several times with acetone and hexane. The particles on the filter were recovered by sonication with *tert*-butyl alcohol at ≈45 °C (ASU-20; AS ONE Corporation, Osaka, Japan).

Determination of Particle and Aggregate Yields. Particle and aggregate yields were calculated based on dry weight by using the following equations

$$\text{Yield}_{\text{particle}} = \frac{M_{\text{particle}}}{C_{\text{solution}}V_{\text{solution}}} \tag{1}$$

$$\text{Yield}_{\text{aggregate}} = \frac{M_{\text{aggregate}}}{C_{\text{solution}}V_{\text{solution}}} \tag{2}$$

where Yield$_{\text{particle}}$ and Yield$_{\text{aggregate}}$ (unitless) are the yield of the generated particles and aggregates, respectively; M_{particle} (mg) is the dry weight of the generated particles; $M_{\text{aggregate}}$ (mg) is the dry weight of the generated aggregates; C_{solution} (mg·mL^{-1}) is the concentration of LDPE in the feedstock solution; and V_{solution} (mL) is the volume of the polymer solution injected. Particles collected on the membrane filter and aggregates collected on the 0.25 mm mesh stainless-steel net were dried by vacuum drying and weighed on an electronic balance. Polymer not accounted for by the particles and aggregates was considered to have been dissolved in the mixture solution or otherwise been lost during the experiment by adhering to the syringe or stir bar. Particle and aggregate masses were used to calculate the suspension density of the polymer in the dispersion.

Particle Size Distribution and Shape Analysis. Images of individual particles were collected under a scanning electron microscope (SEM) and used for analysis of particle size and shape. Particles dispersed in *tert*-butyl alcohol (≈0.1%) at ≈45 °C were loaded onto a polished aluminum stub at room temperature, and the solvent was immediately evaporated with a gentle stream of air. The sample on the stub was then vacuum dried at room temperature for 10 min. Prior to SEM analysis, all samples were sputter-coated with platinum by using an auto-fine coater (JEC-3000FC; JEOL Ltd., Tokyo, Japan) at 10 mA for 1.5–2.0 min. Samples were imaged with a field-emission SEM (JSM-7800F, JEOL Ltd., Tokyo, Japan) in secondary electron imaging mode at an accelerating voltage of 5.0 kV.

SEM images of 90 particles (30 particles from each of three different regions on the stub) were used for shape analysis. Thirty particles is the sample size generally considered sufficient to get an approximation to a normal distribution.[21] Images were taken one by one at a magnification of 25 000× (31.8 pixels = 100 nm). The maximum Feret's diameter and roundness of each particle were determined by using the ImageJ software (version 1.53c).[22] Feret's diameter was used as an index of particle size. Roundness as a shape factor was determined by using the following equation: $4 \times \text{area}/(\pi \times \text{diameter}^2)$; roundness ranged from 0 to 1, and a value of 1 was considered to represent a perfect circle.

Calculation of Growth and Nucleation Rates. To obtain some insights into the mechanisms underlying the formation of particles of different sizes, a simple population balance model was used to represent the particle size distribution. We assumed that the dispersion was at steady-state during injection of the feedstock solution because the amount of polymer used was low (0.1–4% in the feedstock

solution, w/v, and 0.004–0.016% in the dispersion, w/v). Residence time (τ [s]) was assumed to correspond to the time taken to inject the feedstock solution into the antisolvent.
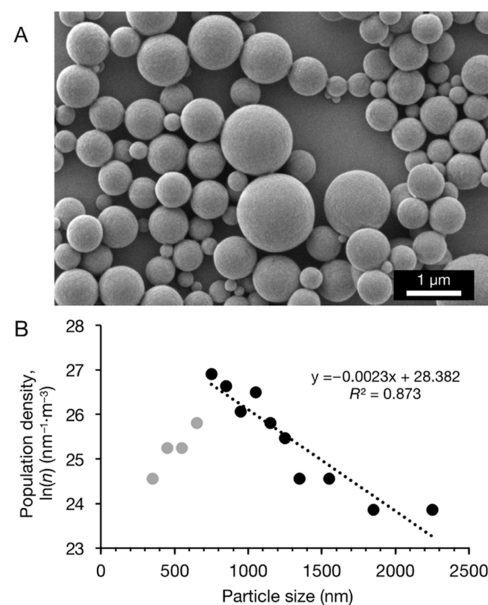
The population density distribution of each sample was calculated from the particle size distribution and was then analyzed by using a simple population balance model, defined as eq 1[19,23]

$$\ln(n) = \ln\left(\frac{B}{G}\right) - \frac{L}{G\tau'} \tag{3}$$

where n (nm^{-1}·m^{-3}) is the population density, L (nm) is the particle diameter, G (nm·s^{-1}) is the particle growth rate, and B (s^{-1}·m^{-3}) is the particle nucleation rate. The relationship between population density and particle diameter was fitted by using the linear least-squares technique for minimizing the sum of squared residuals.

■ RESULTS AND DISCUSSION

Spherical nano-microscale particles were obtained across the entire range of experimental conditions examined in the present study, as confirmed by SEM images. Figure 2A shows a


Figure 2. (A) Representative SEM image and (B) population density distribution of LDPE particles obtained by using 2 mL of feedstock solution at a concentration of 10 mg·mL^{-1}. Particles smaller than the peak of the population density (in gray) were excluded from the calculation of the growth and nucleation rates.

representative SEM image of particles obtained with 2 mL of feedstock solution at a concentration of 10 mg·mL^{-1}. Using the SEM image obtained under each experimental condition, particle sizes were measured, and population density distributions were calculated (Figure 2B). Growth and nucleation rates were determined according to the population balance equation (eq 1). The population density distributions in all of the experiments were unimodal, and particles smaller than the peak population density were excluded from the calculation of growth and nucleation rates.

Effects of Polymer Concentration in the Feedstock Solution. Particle and aggregate yields, mean particle roundness, and mean particle diameter as functions of the concentration of polymer in the feedstock solution are shown

in Figure 3. The particle yield was greater than 80% at feedstock concentrations up to 10 mg·mL^{-1}, after which the
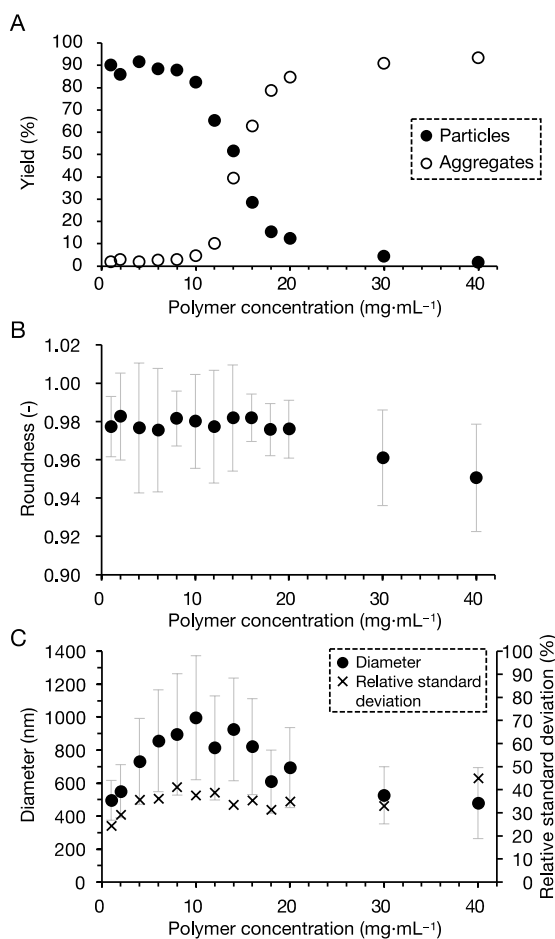
Figure 3. (A) Particle and aggregate yields, (B) mean particle roundness, and (C) mean particle diameter and its relative standard deviation as functions of the concentration of polymer in the feedstock solution during nanoprecipitation of LDPE. Error bars indicate standard deviations.

yield sharply decreased with increasing polymer concentration (Figure 3A). The opposite trend was observed for aggregates. Figure S2 shows a photograph and SEM images of a representative aggregate. The aggregates appeared to have formed as a fusion of several particles, indicating that the aggregates were made of particles dispersed in the antisolvent after injection of the feedstock solution. Particle roundness was around 0.98 at polymer concentrations up to 20 mg·mL^{-1} and was slightly lower at polymer concentrations of 30 mg·mL^{-1} (0.96) and 40 mg·mL^{-1} (0.95) (Figure 3B). These roundness values were high enough for us to consider all of the particles obtained to be spherical.[13]

The mean particle diameter increased linearly from 496 to 997 nm when the polymer concentration was increased from 1 to 10 mg·mL^{-1} (Figure 3C). This increase of particle size can be explained by the fact that the growth rate increased and the nucleation rate decreased in the same polymer concentration range (Figure 4). Thus, up to a polymer concentration of 10 mg·mL^{-1}, the increase in the degree of supersaturation caused by the increase of polymer concentration promoted particle growth rather than nucleation, resulting in an increase in the consumption of polymer for particle growth and a decrease in
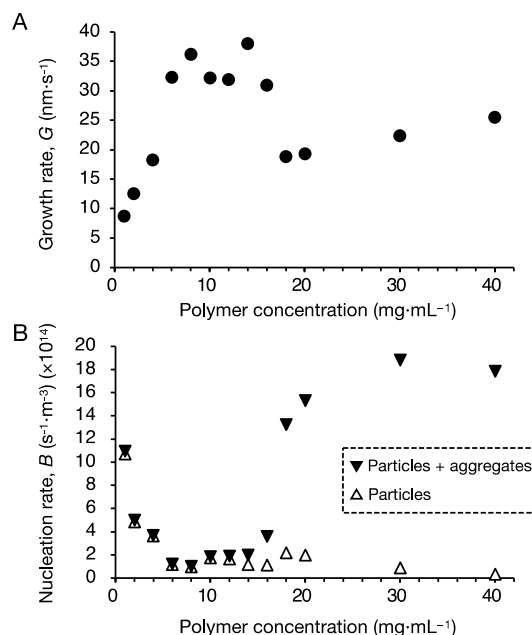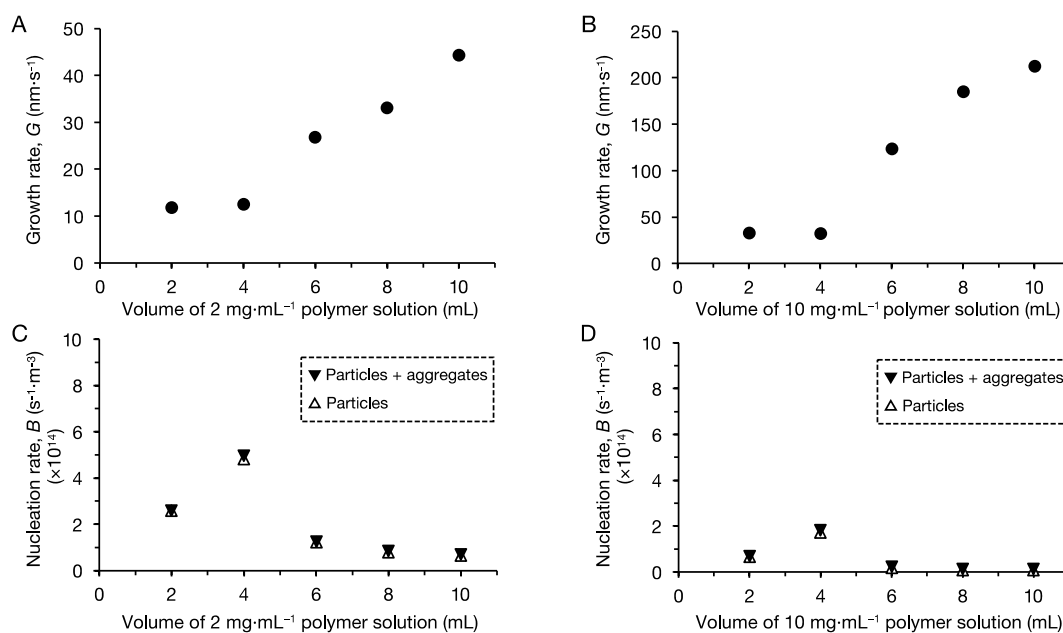

Figure 4. (A) Growth rate and (B) nucleation rate as functions of the concentration of polymer in the feedstock solution during nanoprecipitation of LDPE.

the consumption of polymer for particle nucleation. Although the nucleation rate generally increases with increasing supersaturation, we observed a decrease in the nucleation rate with increasing supersaturation in the polymer concentration range up to 10 mg·mL^{-1}. A possible explanation for this decrease could be that the particle growth caused by precipitation of the polymer was able to proceed without solute crystallization because the temperature of the system at the time of injection of the feedstock solution into the antisolvent was above the melting temperature of the LDPEs; therefore, particle growth was preferentially enhanced with increasing supersaturation, resulting in a decrease in nucleation rate. At polymer concentrations from 10 to 40 mg·mL^{-1}, the mean particle diameter gradually decreased until it was 479 nm at the highest polymer concentration (Figure 3C). At higher polymer concentrations (18–40 mg·mL^{-1}), the growth rate was decreased to less than that from 10 to 16 mg·mL^{-1} (Figure 4A). No clear trend was observed for the nucleation rate calculated only from the density of suspended particles alone at polymer concentrations from 10 to 40 mg·mL^{-1} (Figure 4B). However, because the aggregates were formed from individual particles, ignoring the aggregates likely resulted in under-estimation of the number of particles generated. Therefore, nucleation rates were calculated by using the suspension density of the sum of particles and aggregates and were found to increase and then reach a plateau in the polymer concentration range of 10–40 mg·mL^{-1} (Figure 4B). The suggestion here is that the nucleation rate gradually exceeded the growth rate as the polymer concentration was increased over 10 mg·mL^{-1}, and that this increase in the nucleation rate resulted in a lower amount of polymer available for the growth of individual particles. As a result, particle size was reduced, and the high nucleation rate caused aggregation of the particles, resulting in a reduction of particle yield. The relative standard deviation of particle size was increased from 24 to 36% when the polymer concentration was increased from 1 to 4 mg·mL^{-1}, but no clear trend was observed at polymer
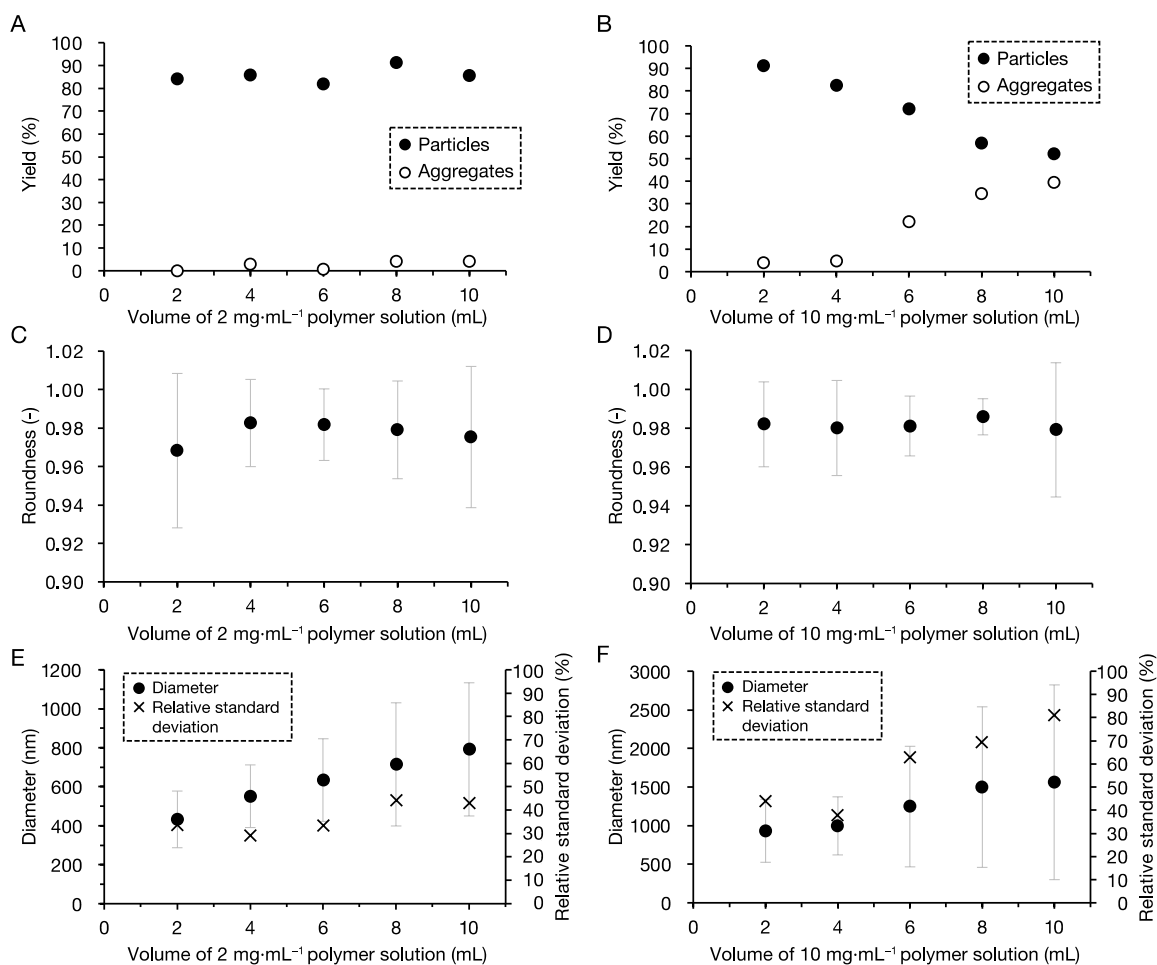
Figure 5. (A,B) Particle and aggregate yields, (C,D) mean particle roundness, and (E,F) mean particle diameter and its relative standard deviation as functions of the volume of feedstock solution used during nanoprecipitation of LDPE. The concentration of polymer in the feedstock solution was 2 or 10 mg·mL^{-1}. Error bars indicate standard deviations.

Figure 6. (A,B) Growth and (C,D) nucleation rates of LDPE nanoprecipitation as functions of the volume of feedstock solution used during nanoprecipitation of LDPE. The concentration of polymer in the feedstock solution was 2 or 10 mg·mL^{-1}.

concentrations higher than 4 mg·mL^{-1} (Figure 4A). This is consistent with the standard deviation of the particle size distribution, which tended to be lower when the degree of particle growth was low.

Thus, when the polymer concentration was in the range of 1−10 mg·mL^{-1}, the particle size increased linearly with the polymer concentration. This indicates that particle size may be controlled by adjusting the concentration of polymer in the feedstock solution. In addition, particles could be prepared without the simultaneous generation of aggregates in this concentration range. In contrast, when the concentration of the feedstock solution was above 10 mg·mL^{-1}, the increase in the nucleation rate caused a decrease in particle size, and particle yields decreased due to aggregation.

Effects of the Volume of Injected Feedstock Solution. Particle yields of more than 80% were achieved across the feedstock volume range examined (2−10 mL) when the concentration of polymer in the feedstock solution was 2 mg·mL^{-1}, and negligible amounts of aggregates were produced (Figure 5A). When a 10 mg·mL^{-1} feedstock solution was used, particle yields were again more than 80%, and few aggregates were produced when a low volume of feedstock solution (2−4 mL) was used; however, at higher volumes (6−10 mL), the particle yield decreased and the aggregate yield increased (Figure 5B). The roundness of the particles indicated that spherical particles were produced at both concentrations and at all volumes examined (Figure 5C,D).

The mean particle diameter increased with increasing volume of feedstock solution at both concentrations used (Figure 5E,F). When the 2 mg·mL^{-1} concentration was used, the mean particle diameter increased from 433 to 792 nm with increasing volume. Similarly, when the 10 mg·mL^{-1} concentration was used, the mean particle diameter increased from 933 to 1562 nm with increasing volume. These increases can be explained by increases in the growth rate of the particles (Figure 6A,B). However, only slight changes in the nucleation rate were observed, and these changes were much smaller than those observed in the experiment for polymer concentration (range: 1×10^{14} to 19×10^{14}), and no clear trend was observed (Figure 6C,D). These findings indicate that increasing the volume of the feedstock solution increased the amount of polymer consumed for particle growth. A potential explanation for this is that although the degree of bulk supersaturation increased as the volume of the feedstock solution increased, the same did not occur for the degree of local supersaturation (i.e., the local driving force "pushing out" the polymer solute molecules from the solution), leading to the induction of particle growth rather than nucleation. The relative standard deviation of particle size was in the range of 30−50% when the 2 mg·mL^{-1} concentration was used (Figure 5E). Higher relative standard deviations, 63−81%, were observed when 6−10 mL of a 10 mg·mL^{-1} polymer solution was used (Figure 5F). This trend may be explained by the higher growth rate that was observed when 6−10 mL of a 10 mg·mL^{-1} polymer solution was used (Figure 6B).

We also conducted an experiment to assess the effects on particle diameter of changing the antisolvent composition (i.e., the ratio of xylene to DMSO) due to the addition of the feedstock solution. We prepared 100 mL of DMSO containing 8 mL of xylene as an antisolvent. Injection of 2 mL of the feedstock solution at a concentration of 2 or 10 mg·mL^{-1} generated particles with a mean diameter of 414 ± 90 and 728 ± 253 nm, respectively. These diameters were similar to those

obtained by injection of 2 mL of feedstock solution into 100 mL of DMSO and much smaller than those obtained by injection of 10 mL of feedstock solution into 100 mL of DMSO. Therefore, we concluded that the composition of the antisolvent was not the reason for the increase in particle size.

Together, these results indicate that changing the volume of the feedstock solution changed the particle size by causing an increase in the growth rate of the particles. Therefore, particle size may be controlled by adjusting the volume of the feedstock solution used during nanoprecipitation.

Effects of Suspension Density. The results obtained in the experiments using different concentrations and volumes of feedstock solution were compared as a function of suspension density. Figures 7 and 8 show the yield, roundness, mean particle diameter, growth rate, and nucleation rate of the particles that were prepared at the various concentrations (1−40 mg·mL^{-1}) and volumes (2−10 mL) of feedstock solution at a concentration of 2 or 10 mg·mL^{-1}, as functions of suspension density.

Particle yield was greater than 80% in both cases of varying the polymer concentration or varying the injection volume of feedstock solution up to a suspension density of 0.4 mg·mL^{-1} (Figure 7A). Particle yield decreased rapidly at suspension densities greater than 0.4 mg·mL^{-1} because of the generation of aggregates. The roundness of the particles was around 0.98 at suspension densities up to 1 mg·mL^{-1}, after which slightly lower values were observed (Figure 7B). The mean particle diameter linearly increased with increasing suspension density, and the plots obtained by varying the polymer concentration and those obtained by varying the injection volume of feedstock solution were comparable up to a suspension density of 0.4 mg·mL^{-1} (Figure 7C). However, at suspension densities over 0.4 mg·mL^{-1}, mean particle diameter gradually decreased as the polymer concentration increased. This trend can be explained by a marked increase in nucleation rate (Figure 8C) and no increase in growth rate (Figure 8A), as discussed in the previous section.

Thus, at suspension densities up to 0.4 mg·mL^{-1}, the mean particle diameter could be controlled by adjusting the suspension density, and the particles could be prepared without generating aggregates and with consistent roundness.

At suspension densities up to 0.4 mg·mL^{-1}, the relative standard deviation of particle size was in the range of 20−50% (Figure 7D). The relative standard deviation of the particle size distribution was substantially larger than that reported for monodisperse particles (e.g., the relative standard deviation of particle size < 5%[24,25]). To obtain monodispersed particles, size fractionation of the prepared particles, such as filtering, is required.

■ CONCLUSIONS

Here, we explored how adjusting the concentration or volume of the feedstock solution affected the yield, roundness, and diameter of LDPE particles prepared by nanoprecipitation. The mechanism of particle formation was also examined by calculating particle growth and nucleation rates.
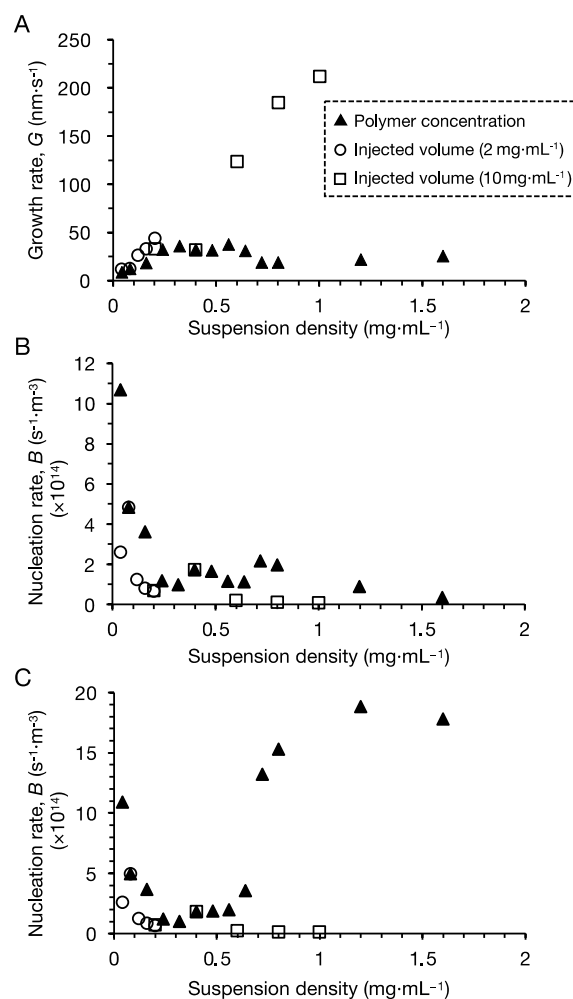
Increasing the concentration of the feedstock solution in the range of 1−10 mg·mL^{-1} resulted in an increase in growth rate and a decrease in nucleation rate, resulting in an increase in particle diameter. Similarly, increasing the volume of the feedstock solution resulted in an increase in growth rate and an increase in particle diameter across the volume range examined (2−10 mL). The change in particle size was linearly correlated
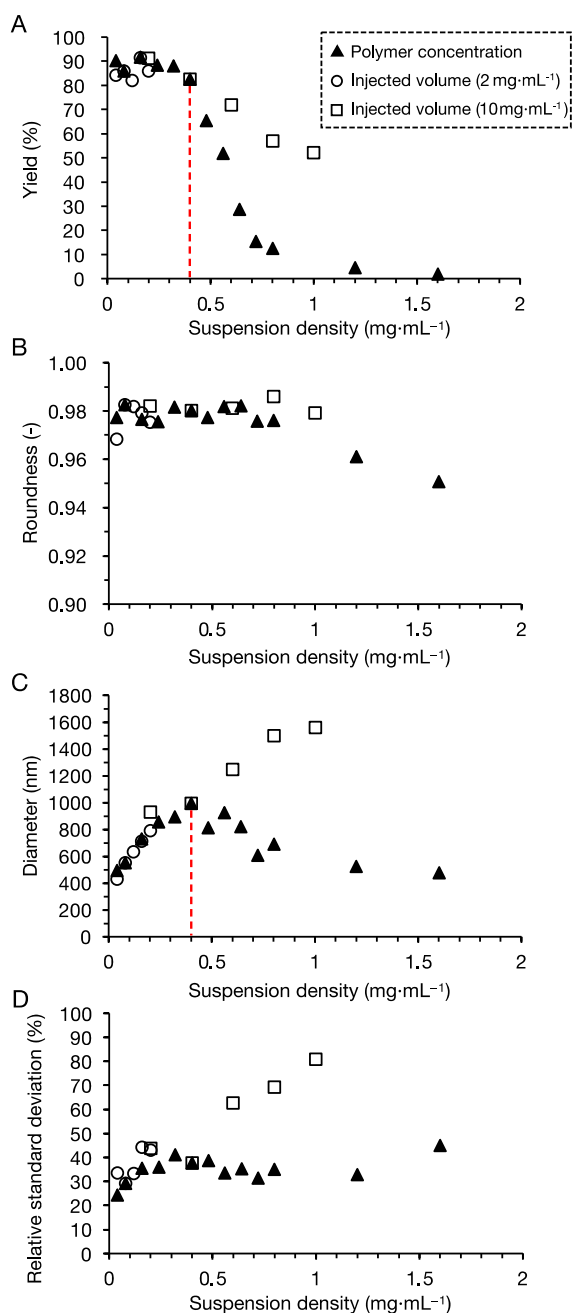
Figure 7. (A) Yield, (B) roundness, (C) mean diameter, and (D) relative standard deviation of diameter of LDPE particles prepared with different concentrations of feedstock solution ($1-40$ mg·mL^{-1}) or with different injection volumes ($2-10$ mL) of feedstock solution at a concentration of 2 or 10 mg·mL^{-1}, as functions of suspension density. Red lines indicate a suspension density of 0.4 mg·mL^{-1}.

Figure 8. (A) Growth rate, (B) nucleation rate calculated from the suspension density of particles alone, and (C) nucleation rate calculated from the suspension density of particles and aggregates, for particles prepared with different concentrations of feedstock solution ($1-40$ mg·mL^{-1}) or with different injection volumes ($2-10$ mL) of feedstock solution at a concentration of 2 mg·mL^{-1} or 10 mg·mL^{-1}, as functions of suspension density.

with the suspension density of the dispersion up to a suspension density of 0.4 mg·mL^{-1}. Thus, under the present conditions, suspension density was indicated to be a universal preparation factor for particle size if the suspension density is 0.4 mg·mL^{-1} or lower.

NP particles of various sizes prepared by nanoprecipitation could be useful tools for examining the risks of NPs. However, the present approach only afforded particles with a mean diameter of 432 nm (when 2 mL of feedstock solution at a concentration of 2 mg·mL^{-1} was used) or larger, and the particle size distributions were large. Further studies are

needed to explore the preparation of smaller NP particles with a narrower size distribution. In addition, the development of scale-independent methods (e.g., a continuous flow method using a microreactor) would facilitate stable particle production. The present results provide a basis for these future studies.

■ ASSOCIATED CONTENT

Ⓢ Supporting Information

The Supporting Information is available free of charge at https://pubs.acs.org/doi/10.1021/acsomega.2c08233.

Mean diameters of particles prepared with different stirring rates and images of a representative aggregate (PDF)

■ AUTHOR INFORMATION

Corresponding Author

Kosuke Tanaka − *Material Cycles Division, National Institute for Environmental Studies, Tsukuba, Ibaraki 305-8506,*

Japan; ⊙ orcid.org/0000-0002-6357-3637;
Email: tanaka.kosuke@nies.go.jp

Authors

Hidetoshi Kuramochi − *Material Cycles Division, National Institute for Environmental Studies, Tsukuba, Ibaraki 305-8506, Japan;* ⊙ orcid.org/0000-0003-2992-8358

Kouji Maeda − *Department of Chemical Engineering & Materials Science, University of Hyogo, Himeji, Hyogo 671-2201, Japan*

Yusuke Takahashi − *Material Cycles Division, National Institute for Environmental Studies, Tsukuba, Ibaraki 305-8506, Japan*

Masahiro Osako − *Material Cycles Division, National Institute for Environmental Studies, Tsukuba, Ibaraki 305-8506, Japan*

Go Suzuki − *Material Cycles Division, National Institute for Environmental Studies, Tsukuba, Ibaraki 305-8506, Japan;* ⊙ orcid.org/0000-0002-4001-5632

Complete contact information is available at:
https://pubs.acs.org/10.1021/acsomega.2c08233

Notes

The authors declare no competing financial interest.

■ REFERENCES

(1) Andrady, A. L. The plastic in microplastics: A review. *Mar. Pollut. Bull.* **2017**, *119*, 12−22.

(2) Song, Y. K.; Hong, S. H.; Eo, S.; Shim, W. J. The fragmentation of nano- and microplastic particles from thermoplastics accelerated by simulated-sunlight-mediated photooxidation. *Environ. Pollut.* **2022**, *311*, 119847.

(3) Leslie, H. A.; van Velzen, M. J. M.; Brandsma, S. H.; Vethaak, A. D.; Garcia-Vallejo, J. J.; Lamoree, M. H. Discovery and quantification of plastic particle pollution in human blood. *Environ. Int.* **2022**, *163*, 107199.

(4) ter Halle, A.; Jeanneau, L.; Martignac, M.; Jardé, E.; Pedrono, B.; Brach, L.; Gigault, J. Nanoplastic in the North Atlantic Subtropic Gyre. *Environ. Sci. Technol.* **2017**, *51*, 13689−13697.

(5) Mitrano, D. M.; Wick, P.; Nowack, B. Placing nanoplastics in the context of global plastic pollution. *Nat. Nanotechnol.* **2021**, *16*, 491−500.

(6) Gigault, J.; El Hadri, H.; Nguyen, B.; Grassl, B.; Rowenczyk, L.; Tufenkji, N.; Feng, S.; Wiesner, M. Nanoplastics are neither microplastics nor engineered nanoparticles. *Nat. Nanotechnol.* **2021**, *16*, 501−507.

(7) Peng, L.; Fu, D.; Qi, H.; Lan, C. Q.; Yu, H.; Ge, C. Micro- and nano-plastics in marine environment: Source, distribution and threats — A review. *Sci. Total Environ.* **2020**, *698*, 134254.

(8) Yong, C. Q. Y.; Valiyaveettil, S.; Tang, B. L. Toxicity of Microplastics and Nanoplastics in Mammalian Systems. *Int. J. Environ. Res. Public Health* **2020**, *17*, 1509.

(9) Shen, M.; Zhang, Y.; Zhu, Y.; Song, B.; Zeng, G.; Hu, D.; Wen, X.; Ren, X. Recent advances in toxicological research of nanoplastics in the environment: A review. *Environ. Pollut.* **2019**, *252*, 511−521.

(10) Baudrimont, M.; Arini, A.; Guégan, C.; Venel, Z.; Gigault, J.; Pedrono, B.; Prunier, J.; Maurice, L.; Ter Halle, A.; Feurtet-Mazel, A. Ecotoxicity of polyethylene nanoplastics from the North Atlantic oceanic gyre on freshwater and marine organisms (microalgae and filter-feeding bivalves). *Environ. Sci. Pollut. Res.* **2020**, *27*, 3746−3755.

(11) Arini, A.; Gigault, J.; Venel, Z.; Bertucci, A.; Baudrimont, M. The underestimated toxic effects of nanoplastics coming from marine sources: A demonstration on oysters (Isognomon alatus). *Chemosphere* **2022**, *295*, 133824.

(12) Ekvall, M. T.; Gimskog, I.; Hua, J.; Kelpsiene, E.; Lundqvist, M.; Cedervall, T. Size fractionation of high-density polyethylene breakdown nanoplastics reveals different toxic response in Daphnia magna. *Sci. Rep.* **2022**, *12*, 3109.

(13) Tanaka, K.; Takahashi, Y.; Kuramochi, H.; Osako, M.; Tanaka, S.; Suzuki, G. Preparation of Nanoscale Particles of Five Major Polymers as Potential Standards for the Study of Nanoplastics. *Small* **2021**, *17*, 2105781.

(14) Miladi, K.; Sfar, S.; Fessi, H.; Elaissari, A. Nanoprecipitation Process: From Particle Preparation to In Vivo Applications. *Polymer Nanoparticles for Nanomedicines: A Guide for their Design, Preparation and Development*; Vauthier, C., Ponchel, G., Eds.; Springer International Publishing: Cham, 2016, pp 17−53.

(15) Zhao, C.-X.; He, L.; Qiao, S. Z.; Middelberg, A. P. J. Nanoparticle synthesis in microreactors. *Chem. Eng. Sci.* **2011**, *66*, 1463−1479.

(16) Balakrishnan, G.; Déniel, M.; Nicolai, T.; Chassenieux, C.; Lagarde, F. Towards more realistic reference microplastics and nanoplastics: preparation of polyethylene micro/nanoparticles with a biosurfactant. *Environ. Sci.: Nano* **2019**, *6*, 315−324.

(17) Cassano, D.; La Spina, R.; Ponti, J.; Bianchi, I.; Gilliland, D. Inorganic Species-Doped Polypropylene Nanoparticles for Multifunctional Detection. *ACS Appl. Nano Mater.* **2021**, *4*, 1551−1557.

(18) Lee, W. S.; Kim, H.; Sim, Y.; Kang, T.; Jeong, J. Fluorescent Polypropylene Nanoplastics for Studying Uptake, Biodistribution, and Excretion in Zebrafish Embryos. *ACS Omega* **2022**, *7*, 2467−2473.

(19) Mullin, J. W. *Crystallization*, 4th ed.; Mullin, J. W., Ed.; Butterworth-Heinemann: Oxford, 2001.

(20) Zhao, C.; Melis, S.; Hughes, E. P.; Li, T.; Zhang, X.; Olmsted, P. D.; Van Keuren, E. Particle Formation Mechanisms in the Nanoprecipitation of Polystyrene. *Langmuir* **2020**, *36*, 13210−13217.

(21) Brase, C. H.; Brase, C. P. *Understanding Basic Statistics, Enhanced*, 7th ed.; Cengage Learning: Boston, 2016.

(22) Schneider, C. A.; Rasband, W. S.; Eliceiri, K. W. NIH Image to ImageJ: 25 years of image analysis. *Nat. Methods* **2012**, *9*, 671−675.

(23) Randolph, A. D.; Larson, M. A. *Theory of Particulate Processes*, 2nd ed.; Academic Press, New York, 1988.

(24) Choi, C.-H.; Hwang, S.; Jeong, J.-M.; Kang, S.-M.; Kim, J.; Lee, C.-S. Microfluidic synthesis of anisotropic particles from Janus drop by in situ photopolymerization. *Open Biomed. Eng. Lett.* **2012**, *2*, 95−99.

(25) Kim, D.-Y.; Jin, S. H.; Jeong, S.-G.; Lee, B.; Kang, K.-K.; Lee, C.-S. Microfluidic preparation of monodisperse polymeric microspheres coated with silica nanoparticles. *Sci. Rep.* **2018**, *8*, 8525.